

Mathematical Modelling and Simulation of Band Pass Filters Using The Floating Admittance Matrix Method.

SANJAY KUMAR ROY (✉ sanjay.roy@tatasteel.com)

Tata Steel Ltd Jamshedpur <https://orcid.org/0000-0001-9779-4975>

Cherry Bhargava

Lovely Professional University

Kamal Kumar Sharma

LPU: Lovely Professional University

Brahmadeo Prasad Singh

NSUT: Netaji Subhas University of Technology

Research

Keywords: Notch Filters, Band-Pass Filters, Active Filters, Passive Filters, Mathematics model, Floating Admittance Matrix.

Posted Date: April 5th, 2021

DOI: <https://doi.org/10.21203/rs.3.rs-340422/v1>

License:  This work is licensed under a Creative Commons Attribution 4.0 International License.

[Read Full License](#)

Mathematical Modelling and Simulation of Band Pass Filters using the Floating Admittance Matrix Method.

Sanjay Kumar Roy¹, Cherry Bhargava², Kamal Kumar Sharma³, Brahmadeo Prasad Singh⁴
Corresponding Author-Sanjay Kumar Roy, Head (Power Distribution), TATA Steel Ltd, India.
sanjay.roy@tatasteel.com

Abstract:

This article describes the Band Pass Filters mathematical modeling, focusing on solutions using the Floating Admittance matrix method (FAM). The solution using the FAM Method looks superior for any circuit analysis. We are introducing a new strategy resulting in one of the best designs of the Bandpass and the Notch Filters. This document provides compelling reasons for the proposed Process, demonstrates its benefits and many valuable extensions and resources.

Keywords: Notch Filters, Band-Pass Filters, Active Filters, Passive Filters, Mathematics model, Floating Admittance Matrix.

1 Introduction

Active filters and Passive Filters are building blocks of any Electronic and Communication Systems that alter or change the amplitude and/or phase characteristics of a signal versus frequency. Active and Passive Filter are linear circuits that remove unwanted signals such as Noise, Interference, and Distortion from the contaminated input signal. Ideally, Active and Passive Filter alters the various frequency components' associated amplitudes and the phase. The frequency-domain behavior of signals defines a Filter. The transfer function of the filter is the Laplace transform of the output signal to the Input Signal. Filter Circuit, which consists of any Active Devices (Transistors) and Op-amps, in addition to Resistors, Inductors, and Capacitors, is called Active Filter.

On the other hand, a filter circuit designed with passive components, such as Resistors, Capacitors, and Inductors, is called a Passive Filter. The operating frequency range of the filter decides the electronic components used to design the circuit. Hence, the filter can also be further categorized based on the operating frequency of a particular circuit. In signal processing, a band-stop filter or band-reject or notch filter is a circuit that passes almost all frequencies unchanged but attenuates those in a specific range to very low levels. It is

just the opposite of a bandpass filter. The notch filter is designed to stop a very small band of frequencies, is called a band-stop filter with a very narrow stop-band. Other names of the filters include "band limit filter," "T-notch filter," "band-elimination filter," and "band-reject filter."

2 Method

The conventional method of analysis uses one of the most suitable methods from among KCL, KVL, Thevenin's, Norton's, etc., as per the suitability for a particular circuit, whether active or passive. The proposed floating admittance matrix method is unique, and the same can be used for all types of circuits. The complicated network can take advantage of the matrix partitioning technique. The sum property of all elements of any row or any column elements equal to zero provides confidence to proceed further for analysis or reobserve the circuit at the very first equation. This saves time and energy.

We know that the planar spiral type of inductor occupies more space and is associated with the low-quality Factor, which is not used in the filter circuit design. For this reason, paper [1] used simulated inductance to achieve a high-quality factor for RF applications. This paper presents the comparative analysis of active inductor design for high-quality factors at high-frequency applications on the selection of active inductor topologies. Active inductor-based circuits are commonly used in integrated circuits where the inductor's quality factor dominates the performance of the designed circuits. Since the planar spiral inductor occupies a large area and shows a low-quality factor, an active inductor is an excellent option to overcome the spiral inductors' drawbacks. This paper summarizes the analysis and simulation results to select one of the best active inductor topologies to generate high-quality factors for high-frequency applications.

The use of shunt filters for better system performance [2] was discussed in the multi constraints belonging to the domain of multi-objective functions. The main aim is to minimize total harmonic distortion of the load voltage, supply line, and cost minimization.

Paper [3] demonstrates the optimal design technique to effectively utilize cables and transformers for harmonically contaminated voltages and currents, accounting for the frequency-dependent loss of power. The method is especially suitable for a higher current carrying capacity of load. It is shown that HP filters have

dual properties to LP filters in the sense of sensitivity. Among various topologies of BP filters, the best topology was demonstrated in this filter.

The knowledge of the transfer function's characterization gives enough information to decide that the correct functioning of the circuit has been achieved. The variation in the input and output impedances, power supply coupling and uncoupling, variation in the circuit components, and other dynamic behaviors in the filters' structure are essential parameters discussed in detail.

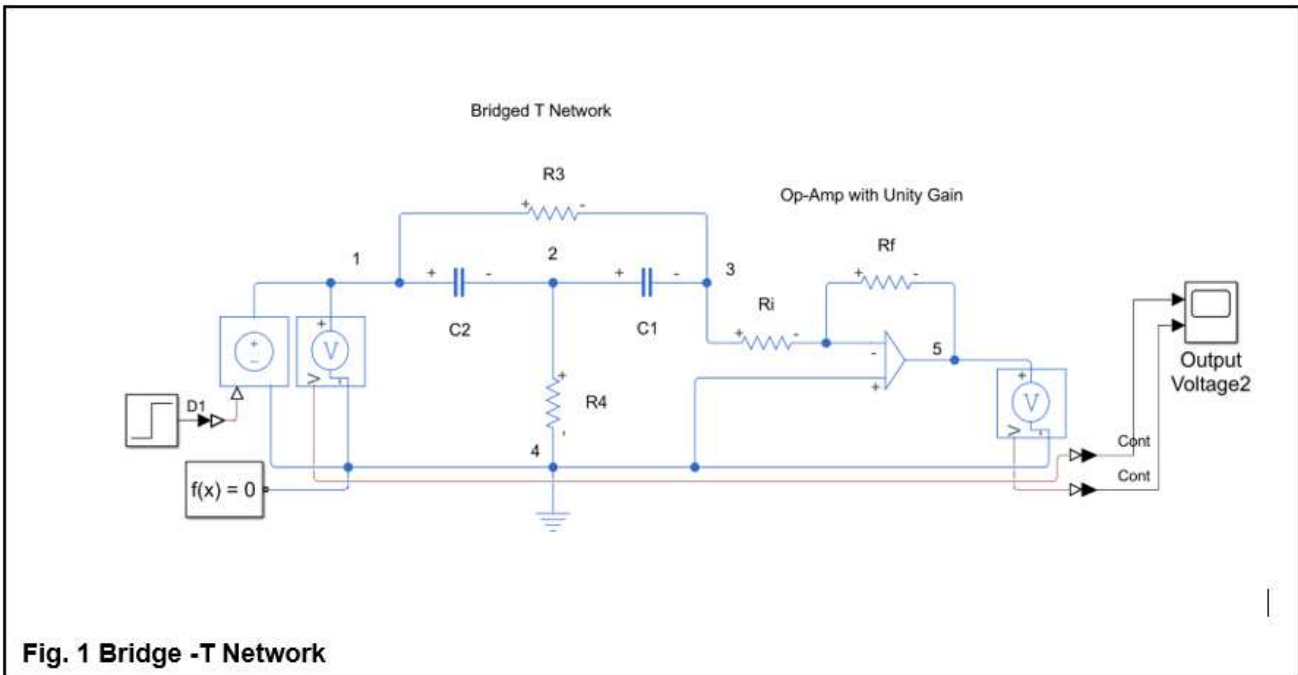
Paper [5] suggests in-depth modelling and design procedure of *LCR* filter, primarily for inverter design used in alternative green energy sources such as a solar system. The MATLAB simulation of PV cell, DC-DC boost converter, and inverter with LCLR filter was also included in the paper.

The heuristic method is supposed to be the easiest and the best for the single tuned passive filters' optimized solution tapping of its essential parameters, which is very difficult. Such techniques provide a reasonable solution in a short time as it uses fewer iterations. The Process called Response Surface Methodology (RSM) [6] was presented to solve issues of paper [5]. This approach seemed to minimize the harmonic distortion in voltage and current in the circuit.

Mathematical modelling based on the admittance matrix model [7-8] uses older elements such as norators, and nullators Papers [9-17] suggested modelling techniques for measuring different parameters three-terminal active devices such as FETs and BJTs. The circuit synthesis using passive components (resistors, inductors, and capacitors) is discussed in detail [18-22]. Desensitization using impedance tapering is being used to design a class-3 circuit with negative feedback. [22-23]. In the negative feedback loops, the RC-section impedance is scaled upwards from the driving source to the negative amplifier input.

Frequency-selective circuits pass the signals of a range of frequencies through it without alteration in the input signal's magnitude. The pass-band filter passes the signal without alteration in the magnitude of the signal to the output port. However, the magnitude of the input signal passed is reduced drastically, ideally to zero value, outside the pass-band. The input currents of such circuits are of no significance, so their transfer functions are not examined. In the subsequent subsection, we will take up some of all types of RC filters, one by one, using a floating admittance matrix approach (FAM).

3 Bridge T-Network: Fig. 1 is a simple circuit of the RC bridge-T Filter network.



The floating admittance matrix of the bridge-T network without Op Amp in Fig. 1 is written as;

$$\begin{bmatrix} 1 & 2 & 3 & 4 \\ G_3 + sC_2 & -sC_2 & -G_3 & 0 \\ -sC_2 & sC_1 + sC_2 + G_4 & -sC_1 & -G_4 \\ -G_3 & -sC_1 & G_3 + sC_1 & 0 \\ 0 & -G_4 & 0 & G_4 \end{bmatrix} \begin{bmatrix} 1 \\ 2 \\ 3 \\ 4 \end{bmatrix} \quad (1)$$

The open-circuit voltage transfer function between terminals 3 & 4 and 1 & 4 can be expressed as;

$$A_v|_{14}^{34} = \text{sgn}(3 - 4)\text{sgn}(1 - 4)(-1)^{12} \frac{|Y_{34}^{14}|}{|Y_{14}^{14}|} = \frac{|Y_{34}^{14}|}{|Y_{14}^{14}|} \quad (2)$$

The transmission zero in Eq. (2) is similar to the poles of the closed-loop circuit of Bridge-T Network in Fig.

1.

$$|Y_{34}^{14}| = \begin{vmatrix} -sC_2 & sC_1 + sC_2 + G_4 \\ -G_3 & -sC_1 \end{vmatrix} = s^2 C_1 C_2 + s(C_1 + C_2)G_3 + G_3 G_4 = s^2 + s \frac{(C_1 + C_2)G_3}{C_1 C_2} + \frac{G_3 G_4}{C_1 C_2}$$

$$\begin{aligned} |Y_{14}^{14}| &= \begin{vmatrix} sC_1 + sC_2 + G_4 & -sC_1 \\ G_3 + sC_1 & G_3 \end{vmatrix} = \begin{vmatrix} sC_2 + G_4 & -sC_1 \\ G_3 & G_3 + sC_1 \end{vmatrix} = \begin{vmatrix} sC_2 + G_3 + G_4 & G_3 \\ G_3 & G_3 + sC_1 \end{vmatrix} \\ &= s^2 + s \frac{\{(C_2 + C_1)G_3 + C_1 G_4\}}{C_1 C_2} + \frac{G_3 G_4}{C_1 C_2} \end{aligned}$$

$$A_v|_{14}^{34} = \frac{|Y_{34}^{14}|}{|Y_{14}^{14}|} = \frac{s^2 + s \frac{(C_1 + C_2)G_3 + G_3G_4}{C_1C_2} + \frac{G_3G_4}{C_1C_2}}{s^2 + s \frac{\{(C_2 + C_1)G_3 + C_1G_4\} + G_3G_4}{C_1C_2}} = \frac{s^2 + s \left(\frac{1}{C_1} + \frac{1}{C_2} \right) \frac{1}{R_3} + \frac{1}{C_1C_2R_3R_4}}{s^2 + s \left\{ \left(\frac{1}{C_1} + \frac{1}{C_2} \right) \frac{1}{R_3} + \frac{1}{C_2R_4} \right\} + \frac{1}{C_1C_2R_3R_4}} = \frac{s^2 + sa + \omega_0^2}{s^2 + sb + \omega_0^2} = \frac{s^2 + s \frac{\omega_0}{Q} + \omega_0^2}{s^2 + s \frac{\omega_{01}}{Q} + \omega_0^2}$$

$$\text{Since, } \beta(s)|_{34}^{14} = \frac{1}{A_v|_{14}^{34}}$$

$$A_v|_{14}^{54} = \frac{v_{54}}{v_{14}} = \frac{v_{34}}{v_{14}} \chi \frac{v_{54}}{v_{34}} = \frac{s^2 + s \frac{\omega_0}{Q} + \omega_0^2}{s^2 + s \frac{\omega_0}{Q_1} + \omega_0^2} \chi \left(-\frac{R_F}{R_i} \right) = -\frac{s^2 + s \frac{\omega_0}{Q} + \omega_0^2}{s^2 + s \frac{\omega_0}{Q_1} + \omega_0^2} \text{ for } R_F = R_i \quad (3)$$

The transmission zero in Eq. (3) is similar to the poles of the closed-loop circuit of Fig. 1. Hence, the transmission zero forms the polynomial as;

$$s^2 + s \frac{\omega_0}{Q} + \omega_0^2 = s^2 + sa + \omega_0^2 = s^2 + s \left(\frac{1}{C_1} + \frac{1}{C_2} \right) \frac{1}{R_3} + \frac{1}{C_1C_2R_3R_4} \quad (4)$$

$$\omega_0^2 = \frac{1}{C_1C_2R_3R_4},$$

$$Q = \frac{\omega_0}{a} = \frac{\omega_0}{\left(\frac{1}{C_1} + \frac{1}{C_2} \right) \frac{1}{R_3}} = \frac{\omega_0}{\left\{ \frac{C_1 + C_2}{C_1C_2R_3} \right\}} = \sqrt{\frac{1}{C_1C_2R_3R_4}} \chi \frac{C_1C_2R_3}{C_1 + C_2} = \frac{\sqrt{C_1C_2R_3/R_4}}{C_1 + C_2}$$

$$\text{For } R_3 = R_4 = R \text{ and } C_1 = C_2 = C, Q = \frac{1}{2} = 0.5 \quad (5)$$

The characteristic equation for pole is;

$$s^2 + s \frac{\omega_0}{Q_1} + \omega_0^2 = s^2 + sb + \omega_0^2, \text{ where}$$

$$b = \left\{ \left(\frac{1}{C_1} + \frac{1}{C_2} \right) \frac{1}{R_3} + \frac{1}{C_2R_4} \right\} = \frac{2}{RC} + \frac{1}{RC} = \frac{3}{RC}, \text{ and } \omega_0 = \frac{1}{RC}$$

$$\frac{\omega_0}{Q_1} = \frac{3}{RC} = 3\omega_0, Q_1 = \frac{1}{3}$$

The characteristic equation for pole is now expressed as;

$$s^2 + 3\omega_0s + \omega_0^2 \quad (6)$$

Though there is no need to find out the current transfer ratio, we include both current transfer and power transfer ratios as demanded by the editor. The current transfer function between terminals 3 & 4 and 1 & 4 can be expressed as;

$$A_i|_{14}^{34} = \text{sgn}(3 - 4)\text{sgn}(1 - 4)(-1)^{12} \frac{|Y_{34}^{14}|}{|Y_4^4|} G_L = \frac{|Y_{34}^{14}|}{|Y_4^4|} G_L \quad (7)$$

$$|Y_4^4| = \begin{vmatrix} G_3 + sC_2 & -sC_2 & -G_3 \\ -sC_2 & sC_1 + sC_2 + G_4 & -sC_1 \\ -G_3 & -sC_1 & G_3 + sC_1 \end{vmatrix} = \begin{vmatrix} G_3 + sC_2 & 0 & -G_3 \\ 0 & G_4 & 0 \\ -G_3 & 0 & G_3 + sC_1 \end{vmatrix}$$

$$= G_4\{(G_3 + sC_2)(G_3 + sC_1) - G_3^2\} = G_4s\{sC_1C_2 + G_3(C_1 + C_2)\}$$

$$A_i|_{14}^{34} = \frac{|Y_{34}^{14}|}{|Y_4^4|} G_L = \frac{s^2C_1C_2 + s(C_1 + C_2)G_3 + G_3G_4}{G_4s\{sC_1C_2 + G_3(C_1 + C_2)\}} G_L \quad (8)$$

The power transfer function between terminals 3 & 4 and 1& 4 can be expressed as;

$$A_p|_{14}^{34} = A_v|_{14}^{34} \chi A_i|_{14}^{34} \quad (9)$$

$$A_p|_{14}^{34} = \left\{ \frac{s^2C_1C_2 + s(C_1 + C_2)G_3 + G_3G_4}{s^2C_1C_2 + s\{(C_2 + C_1)G_3 + C_1G_4\} + G_3G_4} \right\} \left\{ \frac{s^2C_1C_2 + s(C_1 + C_2)G_3 + G_3G_4}{G_4s\{sC_1C_2 + G_3(C_1 + C_2)\}} G_L \right\} \quad (10)$$

4 Experimental Verification

The MATLAB Program for the Bridge T Network and its Bode Plot are shown in Fig. 2. It depicts the plot for Amplitude and Phase variation with reference to frequency. The assumed values of resistances and Capacitances are indicated in the programs.

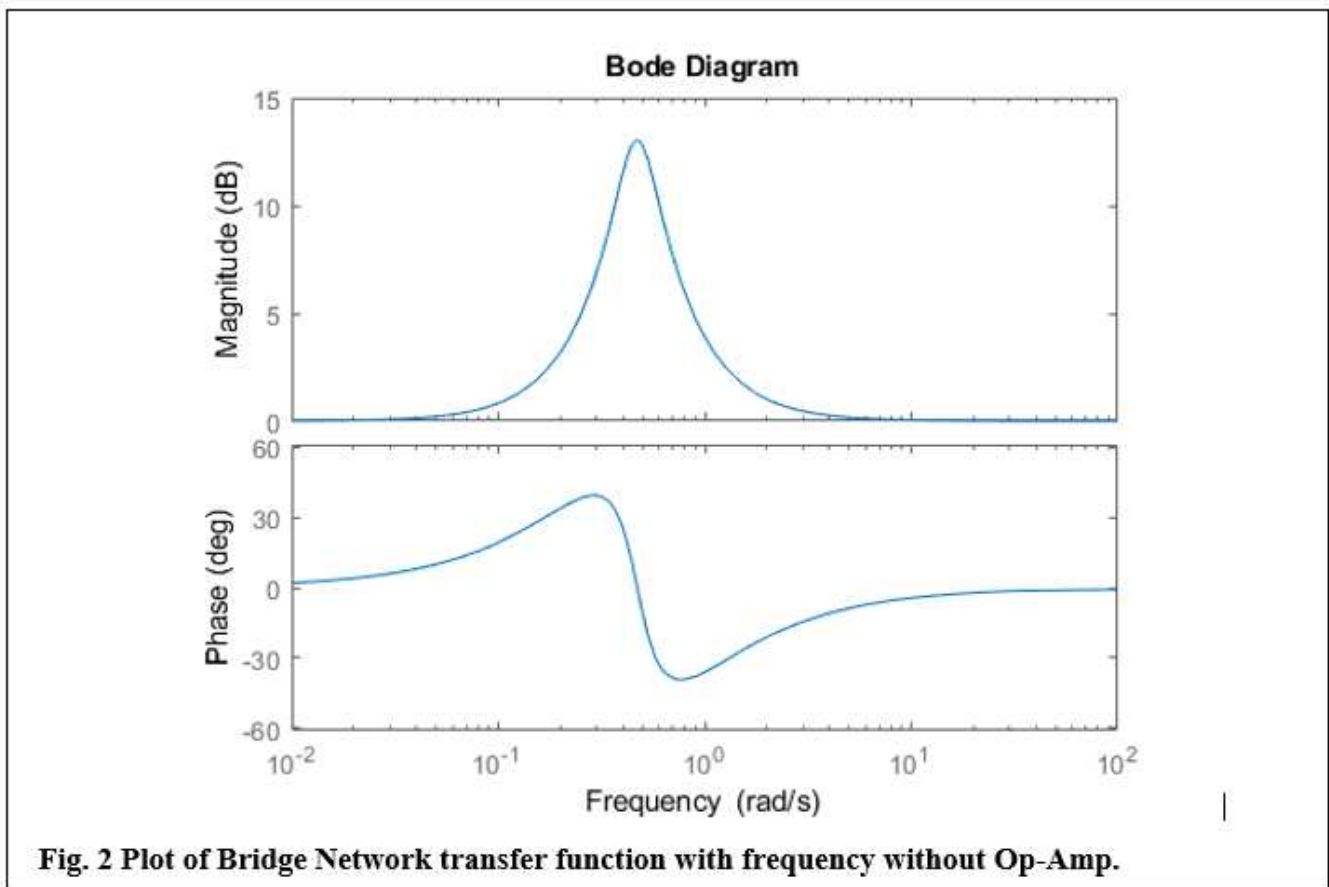
```

r3 = 1500;
r4 = 1500;
c1 = 1000e-6;
c2 = 2000e-6;
A = (1/c1+1/c2)/r3;
B= 1/c1*1/c2*1/r3*1/r4;
C = 1/c1*1/c2*1/r3*1/r4;
D = 1/c1*1/c2*1/r3*1/r4;
num = [1 A B];
den = [1 C D];
GP = tf(num,den);
bode(GP);          s^2 + s + 0.2222
                    GP = -----
                    s^2 + 0.2222 s + 0.2222

```

The continuous-time domain transfer function is plotted in Fig.6.

Figure 2 and 3 are the plot of without and with an inverter that indicates the phase difference of 180 degrees.



The MATLAB Program for the Bridge T Network and its Bode Plot including Op Amp are shown in Fig. 3.

```

r3 = 1500;
r4 = 1500;
c1 = 1000e-6;
c2 = 2000e-6;
A = (1/c1+1/c2)/r3;
B= 1/c1*1/c2*1/r3*1/r4;
C = 1/c1*1/c2*1/r3*1/r4;
D = 1/c1*1/c2*1/r3*1/r4;
num = [1 A B];
den = [1 C D];
GP = -tf(num,den);

```

bode (GP) ;

$$-s^2 - s - 0.2222$$

GP= -----

$$s^2 + 0.2222 s + 0.2222$$

This is the Continuous-time transfer function.

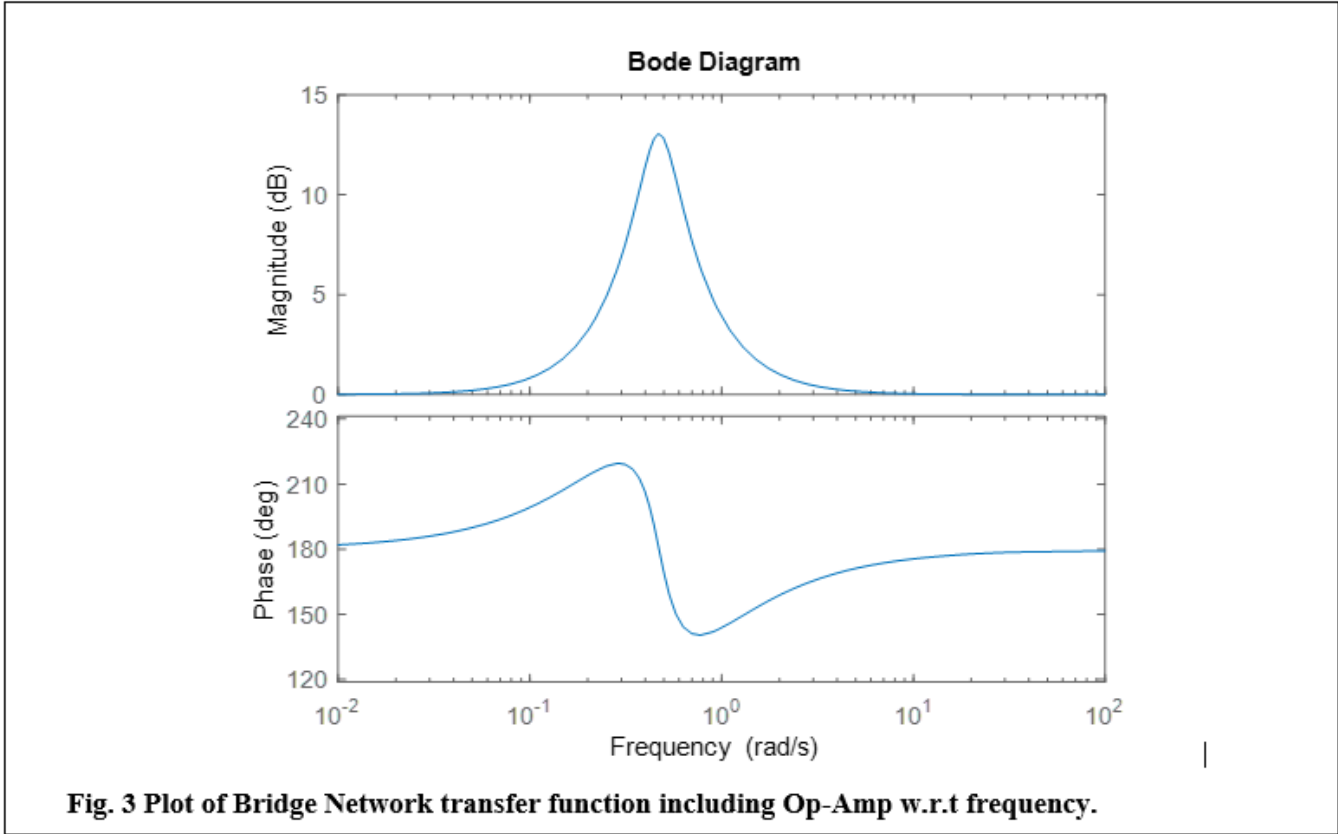


Fig. 3 Plot of Bridge Network transfer function including Op-Amp w.r.t frequency.

The input impedance between terminals 1 & 4 in Fig. 1 is expressed as:

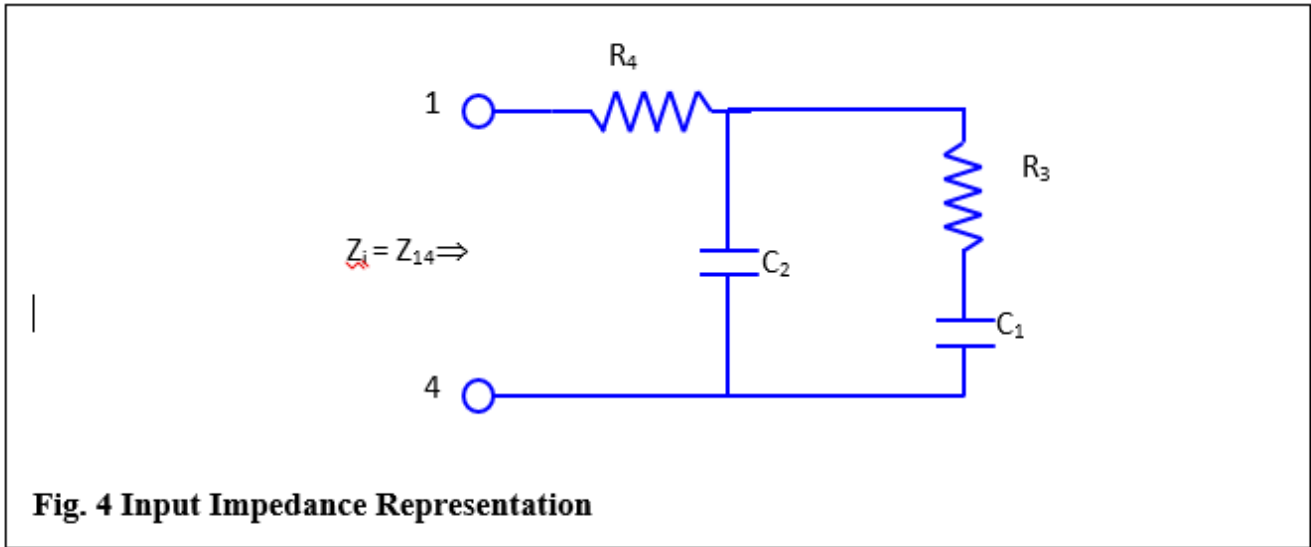
$$Z_{in} = Z_{14} = \frac{|Y_{14}^{14}|}{|Y_4^4|} \Big|_{g_s=0} \tag{11}$$

$$\begin{aligned} |Y_4^4| &= \begin{vmatrix} G_3 + sC_2 & -sC_2 & -G_3 \\ -sC_2 & sC_1 + sC_2 + G_4 & -sC_1 \\ -G_3 & -sC_1 & G_3 + sC_1 \end{vmatrix} = \begin{vmatrix} G_3 + sC_2 & 0 & -G_3 \\ -sC_2 & G_4 & -sC_1 \\ -G_3 & 0 & G_3 + sC_1 \end{vmatrix} \\ &= G_4 \begin{vmatrix} G_3 + sC_2 & -G_3 \\ -G_3 & G_3 + sC_1 \end{vmatrix} = G_4 \begin{vmatrix} sC_2 & -G_3 \\ sC_1 & G_3 + sC_1 \end{vmatrix} = G_4 \{s^2 C_1 C_2 + s(C_1 + C_2)G_3\} \\ &= G_4 s \{sC_1 C_2 + (C_1 + C_2)G_3\} . \end{aligned}$$

$$Z_{in} = Z_{14} = \frac{|Y_{14}^{14}|}{|Y_4^4|} \Big|_{g_s=0} = \frac{s^2 C_1 C_2 + s\{(C_1 + C_2)G_3 + C_1 G_4\} + G_3 G_4}{G_4 s \{sC_1 C_2 + (C_1 + C_2)G_3\}} \tag{12}$$

$$= \frac{1}{G_4} + \frac{sC_1 + G_3}{sC_2(sC_1 + G_3) + C_1 G_3} = \frac{1}{G_4} + \frac{1}{sC_2 + \frac{sC_1 G_3}{sC_1 + G_3}} \tag{13}$$

This equation of input impedance represents in the form of the network shown in Fig. 4 as;



The output impedance between terminals 3 & 4 of Fig. 1 can also be expressed as;

$$R_o = R_{34} = \frac{|Y_{34}^{34}|}{|Y_4^4|_{G_L=0}} \tag{14}$$

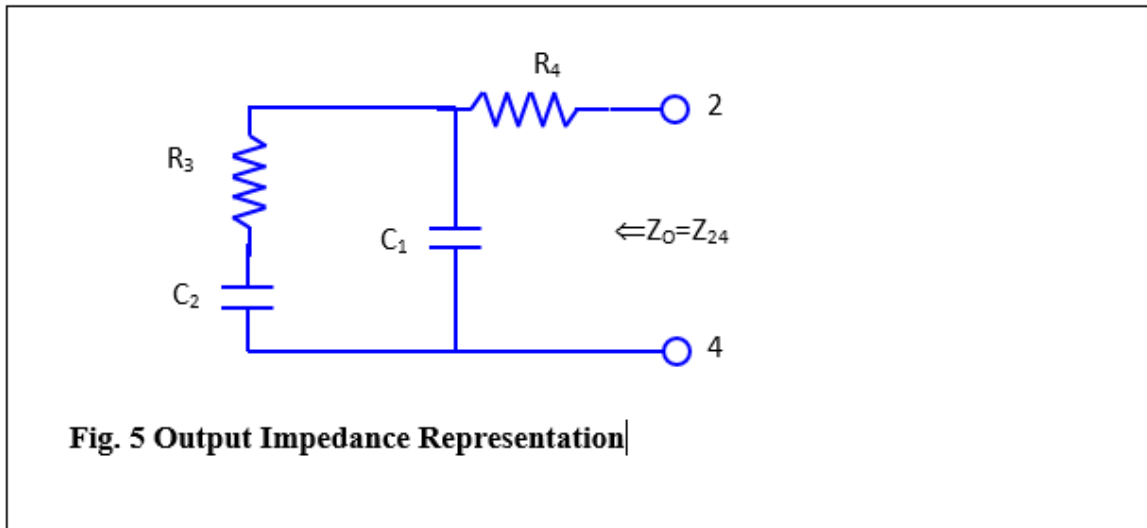
$$|Y_{34}^{34}| = \begin{vmatrix} G_3 + sC_2 & -sC_2 \\ -sC_2 & sC_1 + sC_2 + G_4 \end{vmatrix} = \begin{vmatrix} G_3 + sC_2 & G_3 \\ -sC_2 & sC_1 + G_4 \end{vmatrix}$$

$$= s^2 C_1 C_2 + s(C_1 + C_2)G_3 + sC_2 G_4 + G_3 G_4$$

$$R_o = R_{34} = \frac{|Y_{34}^{34}|}{|Y_4^4|_{G_L=0}} = \frac{s^2 C_1 C_2 + s(C_1 + C_2)G_3 + sC_2 G_4 + G_3 G_4}{G_4 \{s^2 C_1 C_2 + s(C_1 + C_2)G_3\}} \tag{15}$$

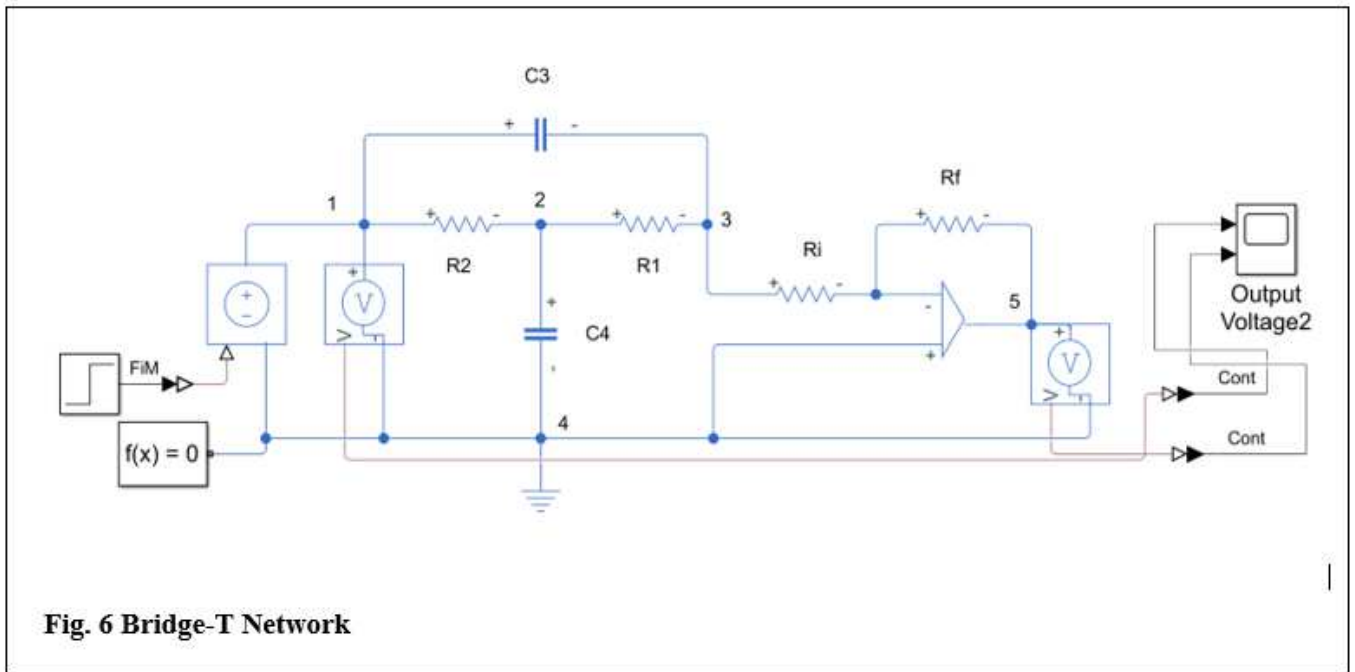
$$= \frac{1}{G_4} + \frac{(sC_2 + G_3)}{s(sC_2 + G_3)C_1 + sC_2 G_3} = \frac{1}{G_4} + \frac{1}{sC_1 + \frac{sC_2 G_3}{sC_2 + G_3}} \tag{16}$$

Eq. (16) represents the circuit in Fig. 5.



5 Second form of Bridge -T Network:

Figure 6 shows the dual form of the Bridge–T networks for realizing the same type of transmission zeros.



The floating admittance matrix for Fig. 6 can be written as;

$$\begin{bmatrix} 1 & 2 & 3 & 4 \\ G_2 + sC_3 & -G_2 & -sC_3 & 0 \\ -G_2 & G_1 + G_2 + sC_4 & -G_1 & -sC_4 \\ -sC_3 & -G_1 & G_1 + sC_3 & 0 \\ 0 & -sC_4 & 0 & sC_4 \end{bmatrix} \begin{bmatrix} 1 \\ 2 \\ 3 \\ 4 \end{bmatrix} \quad (17)$$

The open-circuit voltage transfer function between terminals 3 & 4 and 1 & 4 of Fig. 6 can be expressed [10-11, 13-17] as;

$$A_v|_{14}^{34} = \text{sgn}(3 - 4)\text{sgn}(1 - 4)(-1)^{3+4+1+4} \frac{|Y_{34}^{14}|}{|Y_{14}^{14}|} = \frac{|Y_{34}^{14}|}{|Y_{14}^{14}|} \quad (18)$$

$$\begin{aligned} |Y_{34}^{14}| &= \begin{vmatrix} -G_2 & G_1 + G_2 + sC_4 \\ -sC_3 & -G_1 \end{vmatrix} = G_1G_2 + s(G_1 + G_2)C_3 + s^2C_3C_4 \\ &= s^2 + s \frac{(G_1+G_2)C_3}{C_3C_4} + \frac{G_1G_2}{C_3C_4} \end{aligned}$$

$$\begin{aligned} |Y_{14}^{14}| &= \begin{vmatrix} G_1 + G_2 + sC_4 & -G_1 \\ -G_1 & G_1 + sC_3 \end{vmatrix} = \begin{vmatrix} G_2 + sC_4 & -G_1 \\ sC_3 & G_1 + sC_3 \end{vmatrix} \\ &= s^2C_3C_4 + s\{C_3(G_1 + G_2) + C_4G_1\} + G_1G_2. \end{aligned}$$

$$A_v|_{14}^{34} = \frac{|Y_{34}^{14}|}{|Y_{14}^{14}|} = \frac{s^2 + s \frac{(G_1 + G_2)C_3 + G_1 G_2}{C_3 C_4}}{s^2 + s \frac{\{C_3(G_1 + G_2) + C_4 G_1\} + G_1 G_2}{C_3 C_4}} = \frac{s^2 + s \left(\frac{1}{R_1} + \frac{1}{R_2} \right) \frac{1}{C_4} + \frac{1}{C_3 C_4 R_1 R_2}}{s^2 + s \left\{ \left(\frac{1}{R_1} + \frac{1}{R_2} \right) \frac{1}{C_4} + \frac{1}{R_1 C_3} \right\} + \frac{1}{C_3 C_4 R_1 R_2}} = \frac{s^2 + s \frac{\omega_0}{Q} + \omega_0^2}{s^2 + s \frac{\omega_0}{Q_1} + \omega_0^2}$$

$$A_v|_{14}^{54} = \frac{v_{54}}{v_{14}} = \frac{v_{34}}{v_{14}} \chi \frac{v_{54}}{v_{34}} = \frac{s^2 + s \frac{\omega_0}{Q} + \omega_0^2}{s^2 + s \frac{\omega_0}{Q_1} + \omega_0^2} \chi \left(-\frac{R_F}{R_i} \right) = -\frac{s^2 + s \frac{\omega_0}{Q} + \omega_0^2}{s^2 + s \frac{\omega_0}{Q_1} + \omega_0^2} \text{ for } R_F = R_i \quad (19)$$

In Eq. (19), the transmission zero is similar to the poles of the closed-loop circuit of Fig. 6. Hence, the transmission zero is expressed as;

$$s^2 + s \frac{\omega_0}{Q} + \omega_0^2 = s^2 + as + \omega_0^2 = s^2 + s \left(\frac{1}{R_1} + \frac{1}{R_2} \right) \frac{1}{C_4} + \frac{1}{C_3 C_4 R_1 R_2}$$

$$\text{here, } \omega_0^2 = \frac{1}{C_3 C_4 R_1 R_2} \text{ and} \quad (20)$$

$$Q = \frac{\omega_0}{a} = \sqrt{\frac{1}{C_3 C_4 R_1 R_2}} \chi \frac{1}{\frac{(G_1 + G_2)}{C_4}} = \sqrt{\frac{1}{C_3 C_4 R_1 R_2}} \chi \frac{R_1 R_2 C_4}{R_1 + R_2} = \frac{\sqrt{R_1 R_2 C_4 / C_3}}{R_1 + R_2} \quad (21)$$

$$\text{For } C_3 = C_4 = C, \text{ and } R_1 = R_2 = R, \omega_0 = \frac{1}{RC}, Q = \frac{1}{2}$$

The characteristic equation for poles is;

$$s^2 + s \frac{\omega_0}{Q_1} + \omega_0^2 = s^2 + bs + \omega_0^2,$$

$$b = \left(\frac{1}{R_1} + \frac{1}{R_2} \right) \frac{1}{C_4} + \frac{1}{R_1 C_3} = \frac{3}{RC}, \omega_0 = \frac{3}{RC} = 3\omega_0, Q_1 = \frac{1}{3}$$

The characteristic equation for poles is now expressed as;

$$s^2 + 3\omega_0 s + \omega_0^2 \quad (22)$$

The current transfer function between terminals 3 & 4 and 1 & 4 of Fig. 6 can be expressed [10-11, 13-17] as;

$$A_i|_{14}^{34} = \text{sgn}(3-4) \text{sgn}(1-4) (-1)^{12} \frac{|Y_{34}^{14}|}{|Y_4^4|} G_L = \frac{|Y_{34}^{14}|}{|Y_4^4|} G_L \quad (23)$$

$$\begin{aligned} |Y_4^4| &= \begin{vmatrix} G_2 + sC_3 & -G_2 & -sC_3 \\ -G_2 & G_1 + G_2 + sC_4 & -G_1 \\ -sC_3 & -G_1 & G_1 + sC_3 \end{vmatrix} = \begin{vmatrix} G_2 + sC_3 & 0 & -sC_3 \\ 0 & sC_4 & 0 \\ -sC_3 & 0 & G_1 + sC_3 \end{vmatrix} \\ &= sC_4 \begin{vmatrix} G_2 + sC_3 & -sC_3 \\ -sC_3 & G_1 + sC_3 \end{vmatrix} = sC_4 \begin{vmatrix} G_2 & -sC_3 \\ G_1 & G_1 + sC_1 \end{vmatrix} = sC_4 \{sC_1 G_2 + sC_3 G_1 + G_1 G_3\} \end{aligned}$$

$$A_i|_{14}^{34} = \frac{|Y_{34}^{14}|}{|Y_4^4|} G_L = \frac{s^2 C_3 C_4 + s(G_1 + G_2)C_3 + G_1 G_2}{sC_4 \{sC_1 G_2 + sC_3 G_1 + G_1 G_3\}} G_L \quad (24)$$

The power transfer function between terminals 3 & 4 and 1 & 4 of Fig. 6 can be expressed [10-11, 13-17] as;

$$A_p|_{14}^{34} = A_v|_{14}^{34} \chi A_i|_{14}^{34} = \left\{ \frac{s^2 C_3 C_4 + s(G_1 + G_2)C_3 + G_1 G_2}{s^2 C_3 C_4 + s\{C_3(G_1 + G_2) + C_4 G_1\} + G_1 G_2} \right\} \left\{ \frac{s^2 C_3 C_4 + s(G_1 + G_2)C_3 + G_1 G_2}{sC_4 \{sC_1 G_2 + sC_3 G_1 + G_1 G_3\}} G_L \right\} \quad (25)$$

6 Experimental Verification

The MATLAB Program for the Bridge-T Filter Network and its Bode Plot is shown in Fig. 7. The plot shows Amplitude and Phase variation with reference to frequency. The assumed value of resistances and Capacitances are indicated in the programs.

```

r1 = 1500;
r2 = 1500;
c3 = 1000e-6;
c4 = 2000e-6;
A = (1/c3+1/c3)/r1;
B = 1/c3*1/c4*1/r1*1/r2;
C = A+1/c3*1/r2;
num = [1 A B];
den = [1 C B];
GP = tf(num,den);
bode(GP);
      s^2 + 1.333 s + 0.2222
GP=-----
      s^2 + 2 s + 0.2222

```

The continuous-time domain transfer function is plotted in Fig.7.

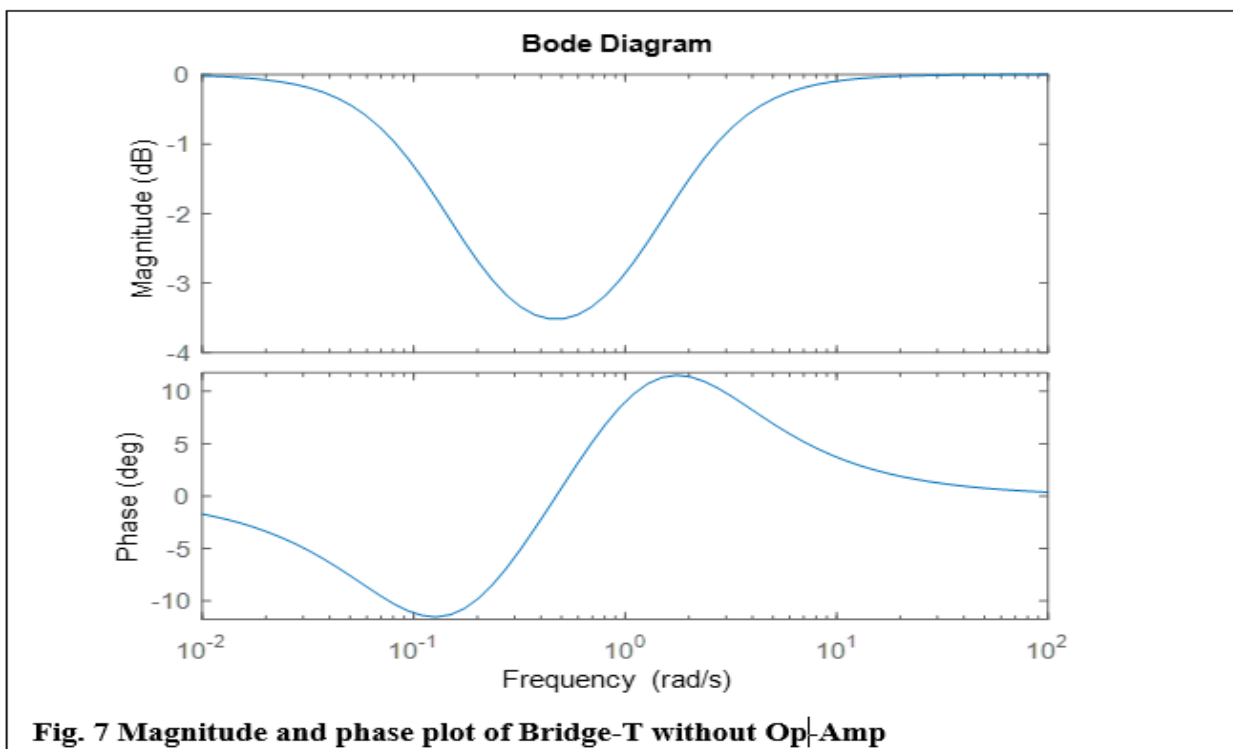


Fig. 7 Magnitude and phase plot of Bridge-T without Op-Amp

The MATLAB Program for the Bridge T Network and Bode Plot is shown in Fig. 6. with Op-Amp.

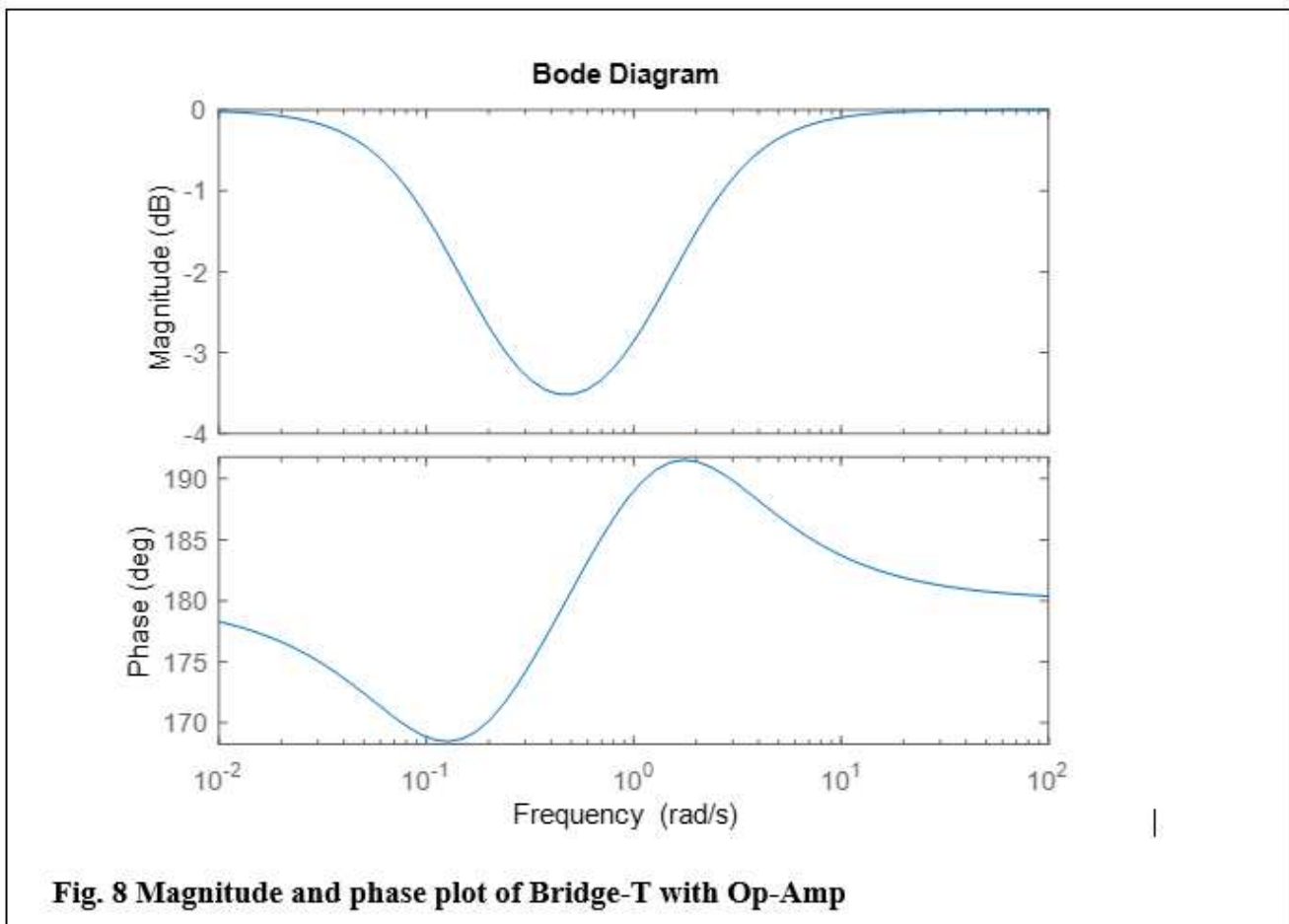
```

r1 = 1500;
r2 = 1500;
c3 = 1000e-6;
c4 = 2000e-6;
A = (1/c3+1/c3)/r1;
B = 1/c3*1/c4*1/r1*1/r2;
C = A+1/c3*1/r2;
num = [1 A B];
den = [1 C B];
GP = -tf(num,den);
bode(GP);

```

$$GP = \frac{-s^2 - 1.333 s - 0.2222}{s^2 + 2 s + 0.2222}$$

This continuous-time domain transfer function is plotted as in Fig.8.



The input impedance between terminals 1 & 4 of Fig. 6 can be expressed [10-11, 13-17] as;

$$Z_{in} = Z_{14} = \frac{|Y_{14}^{14}|}{|Y_4^4|_{g_s=0}} \quad (26)$$

$$|Y_4^4| = \begin{vmatrix} G_2 + sC_3 & -G_2 & -sC_3 \\ -G_2 & G_1 + G_2 + sC_4 & -G_1 \\ -sC_3 & -G_1 & G_1 + sC_3 \end{vmatrix} = \begin{vmatrix} 0 & sC_4 & 0 \\ -G_2 & sC_4 & -G_1 \\ -sC_3 & 0 & G_1 + sC_3 \end{vmatrix}$$

$$= -sC_4\{-(G_1 + sC_3)G_2 - sC_3G_1\} = sC_4\{s(G_1 + G_2)C_3 + G_2G_1\}$$

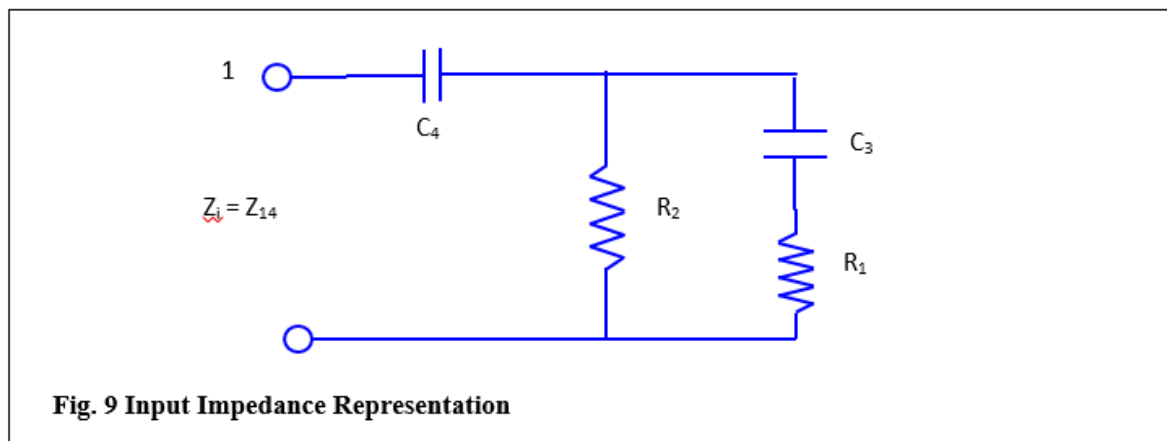
$$Z_{in} = Z_{14} = \frac{|Y_{14}^{14}|}{|Y_4^4|_{g_s=0}} = \frac{s^2C_3C_4 + s\{C_3(G_1 + G_2) + C_4G_1\} + G_1G_2}{sC_4\{s(G_1 + G_2)C_3 + G_2G_1\}}$$

$$= \frac{s\{C_3(G_1 + G_2)\} + G_1G_2}{sC_4\{s(G_1 + G_2)C_3 + G_2G_1\}} + \frac{s^2C_3C_4 + sC_4G_1}{sC_4\{s(G_1 + G_2)C_3 + G_2G_1\}}$$

$$Z_i = Z_{14} = \frac{s^2C_3C_4 + s\{C_3(G_1 + G_2) + C_4G_1\} + G_1G_2}{sC_4\{(G_1 + G_2)C_3 + G_1G_2\}} \quad (27)$$

$$= \frac{1}{sC_4} + \frac{1}{G_2 + \frac{sC_3G_1}{sC_3 + G_1}} = \frac{1}{sC_4} + \frac{1}{G_2 + \frac{sC_3G_1}{sC_3 + G_1}} \quad (28)$$

This input impedance represents in the form of a network shown in Fig. 9.



The output impedance of Fig. 6 between terminals 3 & 4 can be written [10-11, 13-17] as;

$$Z_o = Z_{34} = \frac{|Y_{34}^{34}|}{|Y_4^4|_{G_L=0}} \quad (29)$$

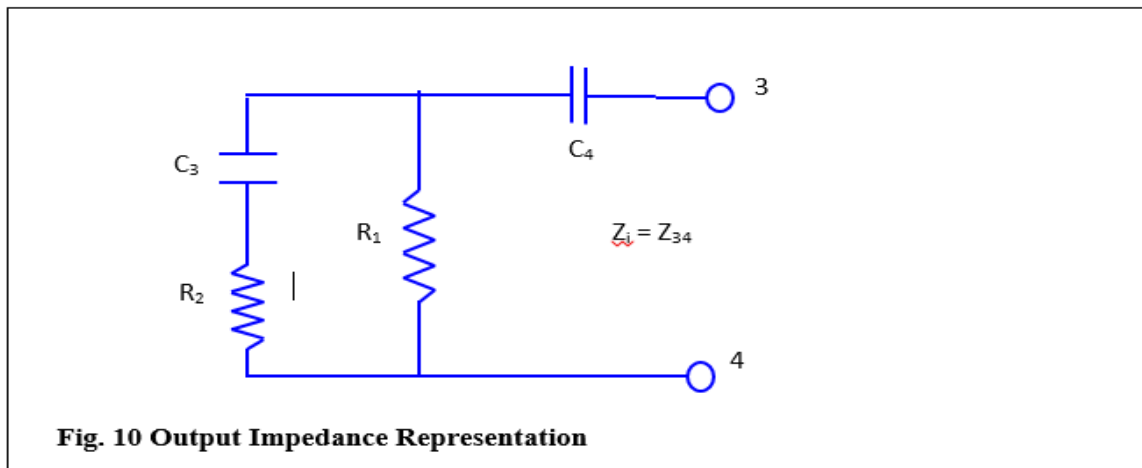
$$|Y_{34}^{34}| = \begin{vmatrix} G_2 + sC_3 & -G_2 \\ -G_2 & G_1 + G_2 + sC_4 \end{vmatrix}$$

$$= (G_1 + G_2)G_2 + G_2sC_4 + sC_3(G_1 + G_2) + s^2C_3C_4 - G_2^2 = s^2C_3C_4 + s\{C_3(G_1 + G_2) + C_4G_2\} + G_1G_2$$

$$Z_o = Z_{34} = \frac{S^2 C_3 C_4 + S\{C_3(G_1 + G_2) + C_4 G_2\} + G_1 G_2}{SC_4\{SC_3(G_1 + G_2) + G_1 G_2\}} \quad (30)$$

$$= \frac{1}{SC_4} + \frac{SC_4(SC_3 + G_2)}{SC_4\{SC_3(G_1 + G_2) + G_1 G_2\}} = \frac{1}{SC_4} + \frac{1}{G_1 + \frac{SC_3 G_2}{SC_3 + G_2}} \quad (31)$$

Figure 10 shows the circuit of output impedance as per equation (31).



7 Results and Discussions:

The plots in Figs. 2, 3, 7, and 8 corroborate the theoretical results obtain. The Floating Admittance Matrix Mathematical Model presented here is so simple that anybody without knowledge of electronics but understanding matrix maneuvering can analyse the circuits to derive all transfer functions. The parameters of devices are known to him/ her. The analysis and then designing any circuit using the floating admittance matrix model is based on pure mathematical maneuvering of matrix elements. The transfer functions are defined as minors' ratio with proper signs, called cofactors of first and or second order. The mathematical modelling using the FAM approach provides leverage to the designer to comfortably adjust their design style at any analysis stage.

8 Conclusions:

The RC filters' response purely depends on the properties of the passive components used, such as R and C. Fundamental characteristics of R and C are associated with the deviations in these components' values based on their tolerances and aging. So, better tolerance may result in lesser deviations in the filter circuit

response. The passive RC filters circuits' response suffers due to lack of precision components used in the circuit tagged with low-Quality Factor, signal loss in the circuit, and dissipation in the Passive components. Incidentally, the selection of precise values of resistances and capacitances with better tolerances yields a better response.

Abbreviation

KCL; Kirchhoff's Current Law, KVL; Kirchhoff's Voltage Law, FAM; Floating Admittance Matrix, HP; High Pass, LP; Low Pass.

Availability of data and materials:

Data sharing does not apply to this article as no datasets were generated for analysis during current studies.

Competing Interest:

No financial and non-financial competing interests exist for this article.

Funding:

No funding agency supports this research work.

Authors contribution:

Author 1 participated in the design and analysis of the manuscript. Authors 2, 3, and 4 participated in the sequence alignment and read and approved the final manuscript.

Author Details:

¹Ph.D. Scholar, Head (Power Distribution), OMQ Division, TATA Steel Ltd India, sanjay.roy@tatasteel.com.

²Associate Professor, Electronics & Communication Engineering, Lovely Professional University, Phagwara, Punjab, (India), cherry.bhargava@lpu.co.in, ³Professor, Electronics & Communication Engineering, Lovely Professional University, Phagwara, Punjab, (India), kamalsharma111@gmail.com, ⁴Professor Adjunct, Electronics & Communication Engineering, Netaji Subhas University of Technology, New Delhi (India), bpsinghgkp@gmail.com.

References:

- [1] Omar Faruq, Md. M. M. Saikat, Md. A. K. Bulbul and Md. Tawfiq Amin: "Comparative Analysis and Simulation of Active Inductors for RF Applications in 90 nm CMOS" 2017 3rd International Conference on Electrical Information and Communication Technology (EICT), 7-9 December 2017, Khulna, Bangladesh.
- [2] Shady H.E. Abdel Aleem, Mohamed T. Elmathana and Ahmed F. Zobaa: "Different Design Approaches of Shunt Passive Harmonic Filters Based on IEEE Std. 519-1992 and IEEE Std. 18-2002". *Recent Patents on Electrical & Electronic Engineering* 2013, 6, 68-75.
- [3] Shady H.E. Abdel Aleem, Murat Erhan Balci, Selcuk Sakar: "Utilization of cables and transformers using passive filters for non-linear loads" *Electrical Power and Energy Systems* 71 (2015) 344–350.
- [4] M. Bogdan, M. Panu: "Lab View Modeling and simulation of the Low pass and High Pass analog filters". 2015 13th International Conference on Engineering of Modern Electric Systems (EMES).
- [5] D. S. Sargar, C. L. Bhattar. "LCLR filter design and modelling for harmonic mitigation in interconnected micro grid system." ISSN: 2319-1163 | ISSN: 2321-7308.
- [6] Selcuk Sakar, Aslan Deniz Karaoglan, Murat Erhan Balci, Shady H. E. Abdel Aleem, Ahmed F. Zobaa.: "Optimal Design of Single-Tuned Passive Filters Using Response Surface Methodology". XII International School on Nonsinusoidal Currents and Compensation, ISNCC 2015, Łagów, Poland.

- [7] Haigh, David G., and Paul M. Radmore. "Admittance matrix models for the nullor using limit variables and their application to circuit design", *IEEE Transactions on Circuits and Systems I: Regular Papers* 53, no. 10 (2006): 2214-2223.
- [8] Vago, I., and E. Hollos. "Two-port models with nullators and norators", *Periodica Polytechnica Electrical Engineering* 17, no. 4 (1973): 301-309.
- [9] Kumar, Pragati, and Raj Senani. "Improved grounded-capacitor SRCO using only a single PFTFN", *Analog Integrated Circuits and Signal Processing* 50, no. 2 (2007): 147-149.
- [10] DBSJ Prasad Rao, B.P. Singh, Dikshitulu Kaluri, "A note on the measurement of FET parameters" *Int. J.*, pp 521-524, vol. 41, 1976.
- [11] B. P. SINGH, "On demand realization of a frequency-dependent negative resistance and an infinite input impedance" *International Journal of Electronics Theoretical and Experimental*, Taylor & Francis, Vol.44, no. 3 (1978): 243-249.
- [12] Chen, Wai-Kai. "Circuit analysis and feedback amplifier theory". CRC Press, 2005.
- [13] Meena Singh, Sanjay Roy, and B. P. Singh, "On Demand Realization of Input and Output Resistances of MOSFET Amplifier". In *American Institute of Physics Conference Proceedings*, vol. 1414, no. 1, pp. 266-270. AIP, 2011.
- [14] B. P. Singh, "A Null Method for Measuring the Parameters of a FET", *Int. J. Electronics*, Vol.44, pp.251-256, Feb.1978, ISSN: 0020-7217.
- [15] B. P. Singh, "Minimum Sensitive FET Filter", *Indian J. Pure & Appl. Phys. (India)*, Vol.20. pp. 389, May 1982, ISSN: 0019-5596.
- [16] B. P. Singh, "Null Method for measuring h-Parameter", *Indian J. Pure & Appl. Phys.*, Vol.16, pp.337-339, 1982, ISSN: 0019-5596.
- [17] B. P. Singh, "Active Bridge for Measurements of the Admittance Parameters of the Transistor", *Indian Journal of Pure & Applied Physics*, Vol. 15, pp. 783, Nov. 1976, ISSN: 0019-5596.
- [18] W. L. Everitt and GE Anner, "Communication Engineering", McGraw-Hill, 1937.
- [19] Darlington, S, "A history of network synthesis and filter theory for circuits composed of resistors, inductors, and capacitors", *IEEE Trans. Circuits and Systems*, vol 31, pp3-13, 1984.
- [20] Vizmuller, P, "RF Design Guide: Systems, Circuits, and Equations", Artech House, 1995, ISBN 0-89006-754-6.
- [21] D. Jurišić, G. S. Moschytz, N. Mijat Faculty of Electrical Engineering and Computing Unska 3 Zagreb 10000, croatia, "low-sensitivity sab bandpass active-RC Filter using impedance tapering", 0-7803-6685-9/01/©2001 IEEE.

Figure Legends:

Fig. 1. Bridge -T Network

Fig. 2 Plot of Bridge Network transfer function with frequency without Op-Amp.

Fig. 3 Plot of Bridge Network transfer function including Op-Amp w.r.t frequency.

Fig. 4 Input Impedance Representation

Fig. 5 Output Impedance Representation

Fig. 6 Bridge-T Network - Second Form

Fig. 7 Magnitude and phase plot of Bridge-T without Op-Amp

Fig. 8 Magnitude and phase plot of Bridge-T with Op-Amp

Fig. 9 Input Impedance Representation

Fig. 10 Output Impedance Representation

Figures

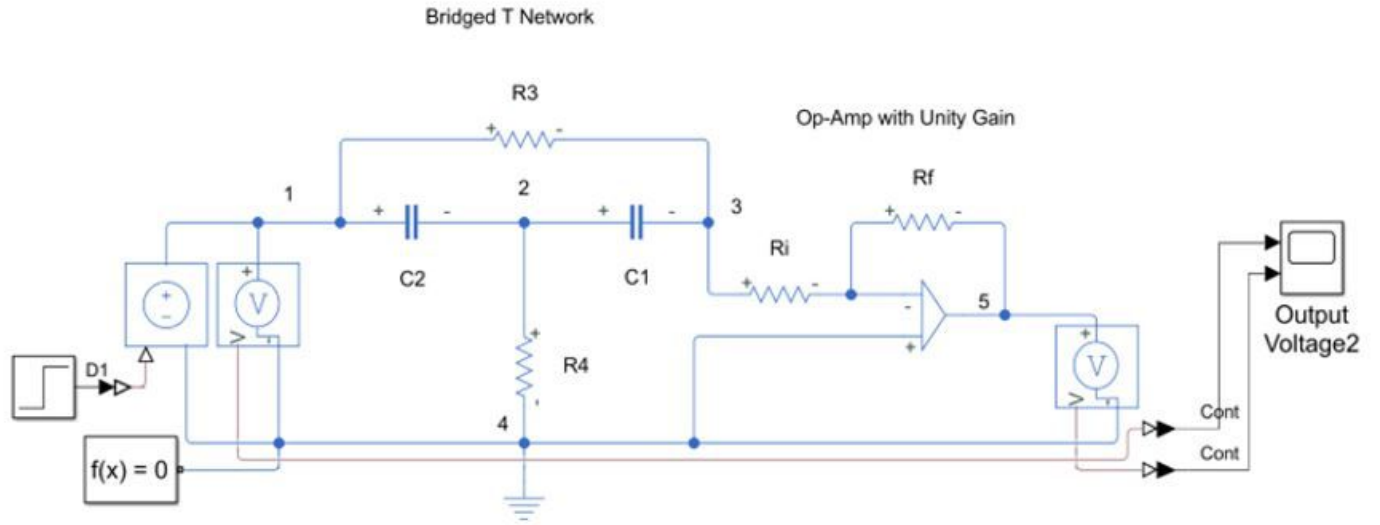


Figure 1

Bridge -T Network

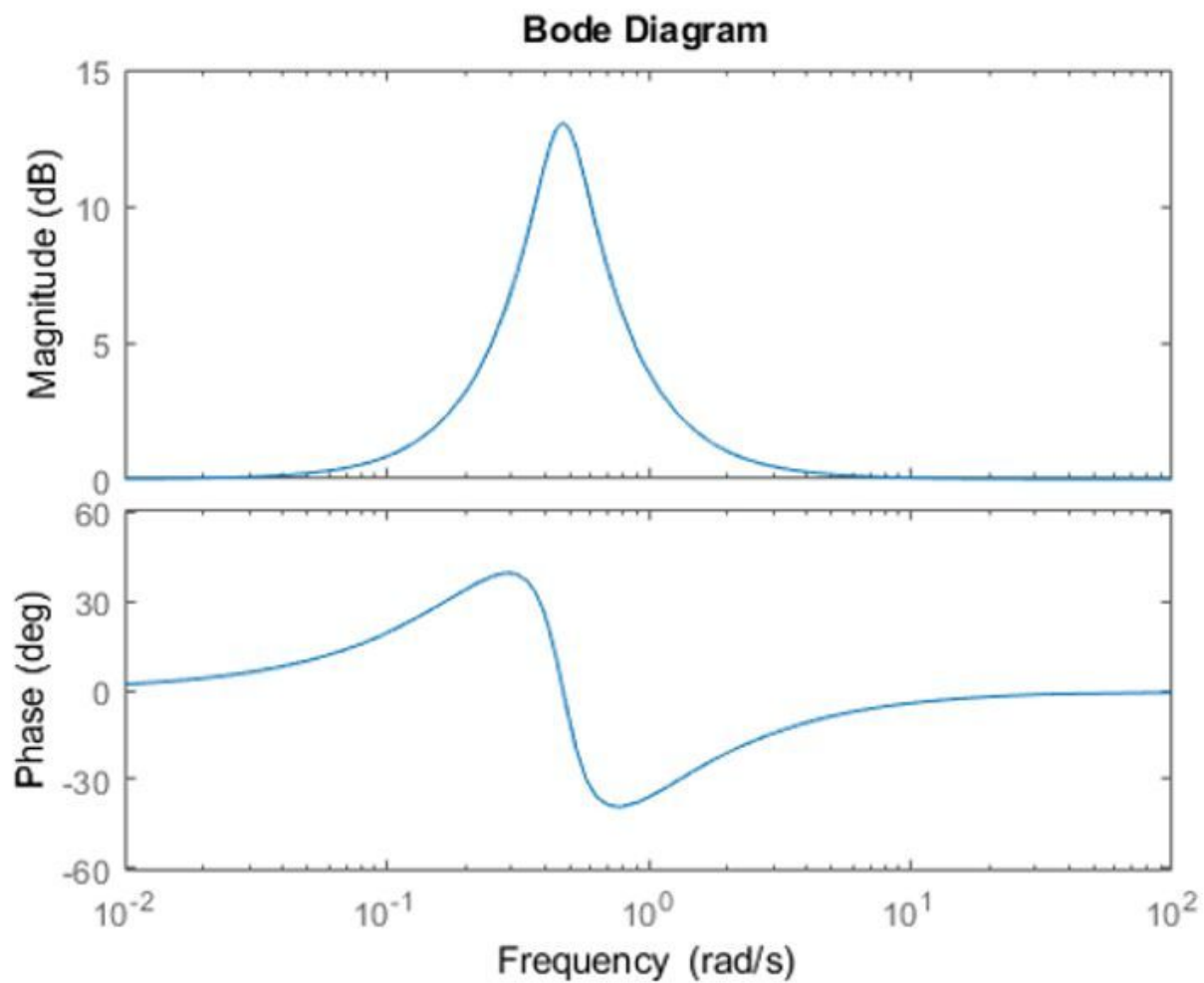


Figure 2

Plot of Bridge Network transfer function with frequency without Op-Amp.

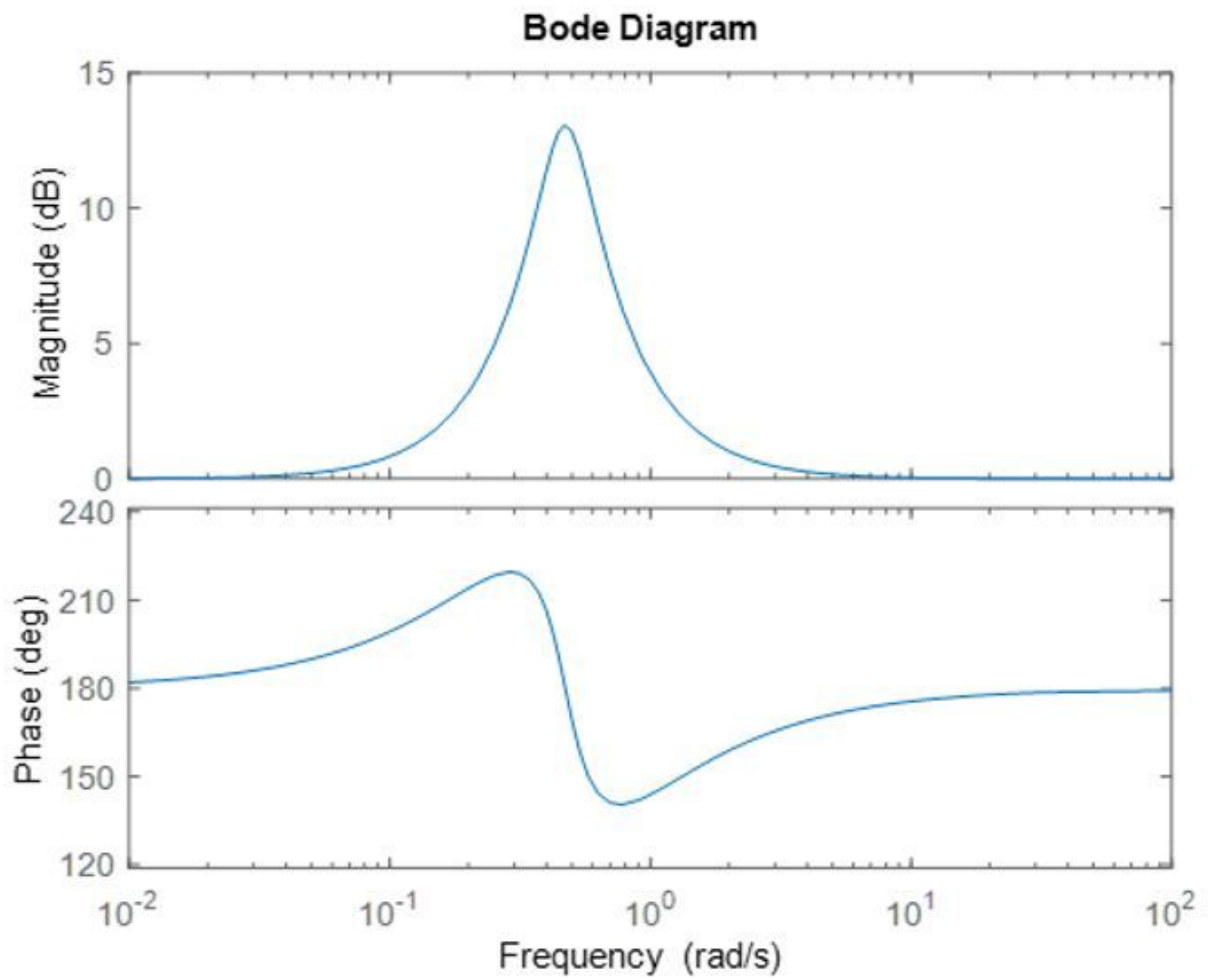


Figure 3

Plot of Bridge Network transfer function including Op-Amp w.r.t frequency.

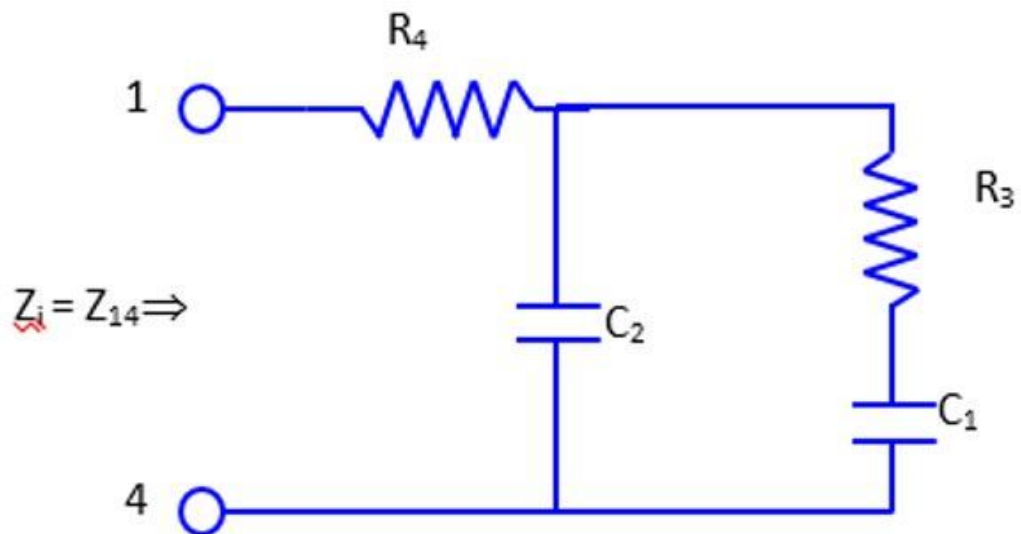


Figure 4

Input Impedance Representation

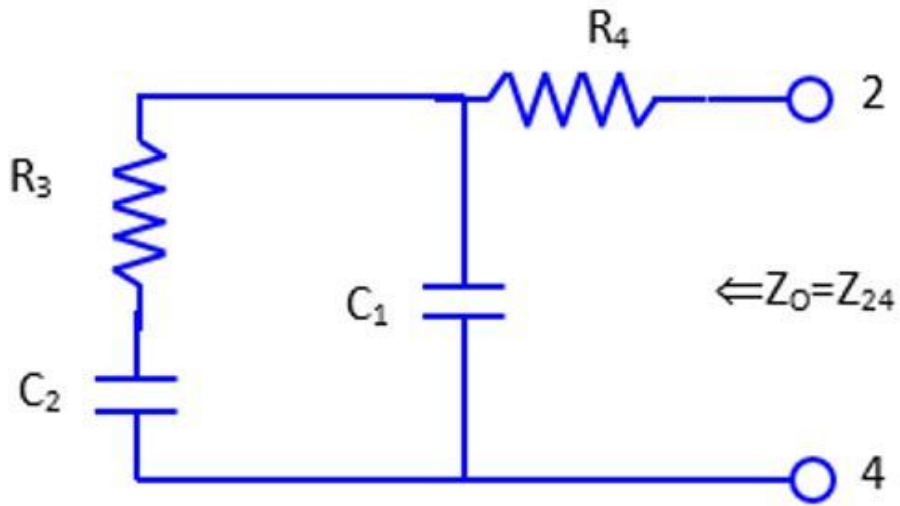


Figure 5

Output Impedance Representation

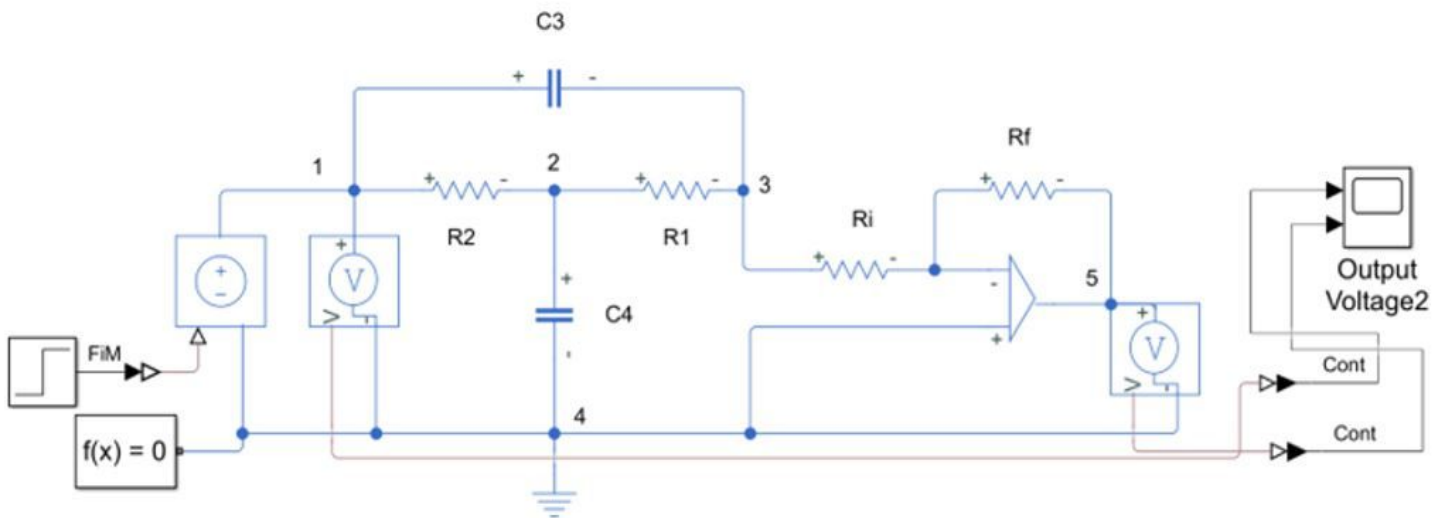


Figure 6

Bridge-T Network - Second Form

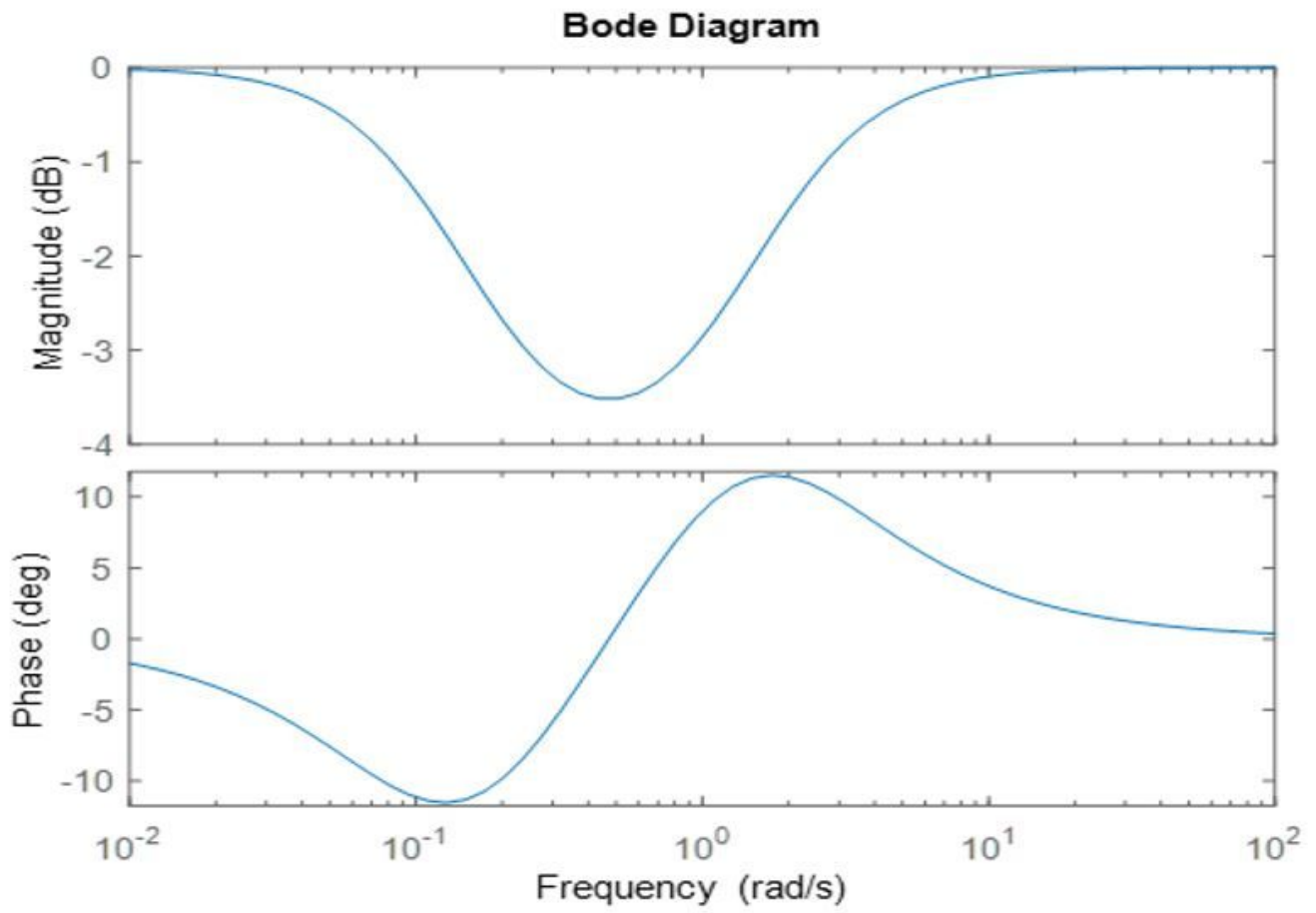


Figure 7

Magnitude and phase plot of Bridge-T without Op-Amp

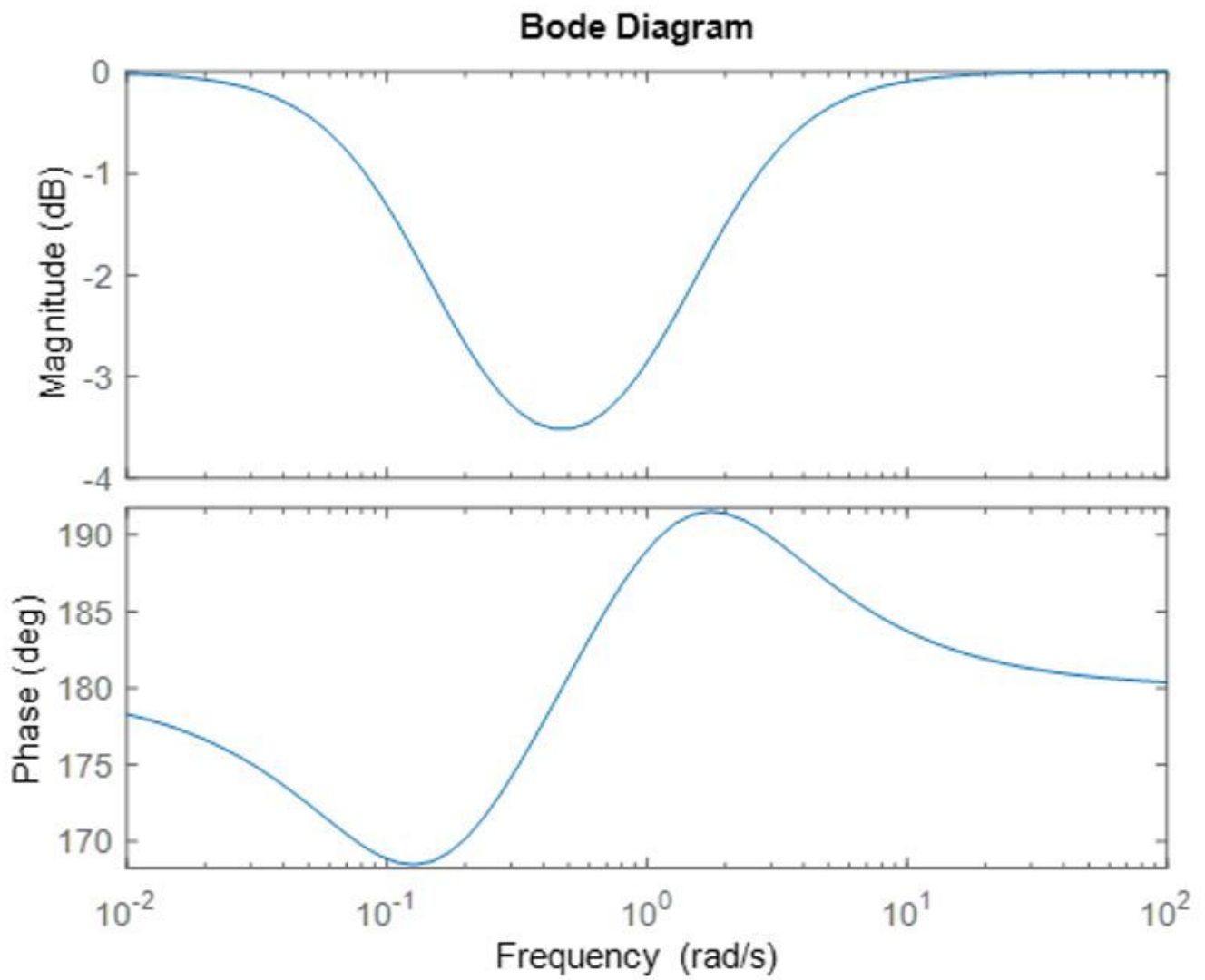


Figure 8

Magnitude and phase plot of Bridge-T with Op-Amp

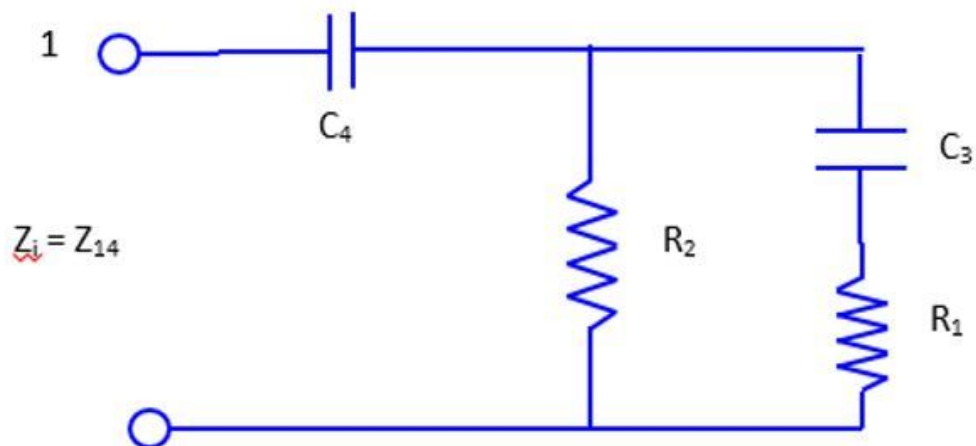


Figure 9

Input Impedance Representation

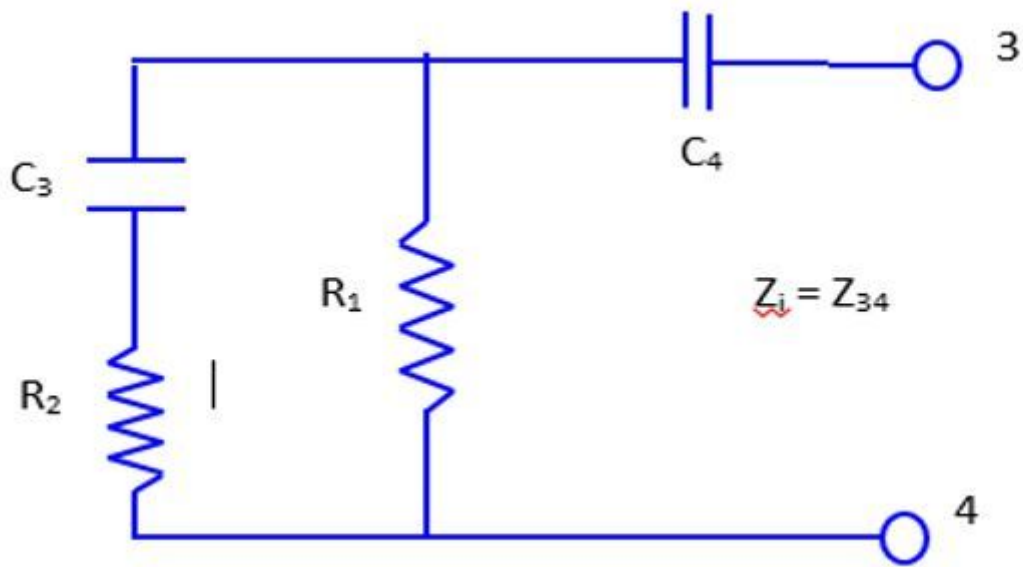


Figure 10

Output Impedance Representation